Magnetically Targeted Drug Transport and Fixation

A.A. Dobre[1], A.M. Morega[1,2], and M. Morega[1]

[1] Faculty of Electrical Engineering, University POLITEHNICA of Bucharest, Bucharest, Romania
[2] "Gheorghe Mihoc – Caius Iacob" Institute of Mathematical Statistic and Applied Mathematics, Romanian Academy

Abstract— **This paper presents a mathematical model and numerical simulation results on transport and targeting of a medical substance carried by magnetic nanoparticles through a high gradient magnetic field. In our study we use simpler yet consistent models for the hemodynamic flow, and more complex, realistic computational domains based on medical images for the iliac arterial branching. The biocompatible drug carrier is injected in the blood. An optimized array of permanent magnets generates the targeting magnetic field, in the process of medication delivery in the region of therapeutic concern.**

Keywords— **magnetic drug targeting, flow – magnetic field interaction, numerical simulation, optimization.**

I. Introduction

Magnetic drug targeting (MDT) is a noninvasive modern technique to reduce the side effects related to the excessive distribution of powerful medication and improve its efficiency. In this therapy, the medication carried by superparamagnetic nanoparticles and injected in the blood stream interacts with an external magnetic field aimed at targeting the drug and fixing it mostly in the region of interest (ROI) for optimal delivery [1-3].

For example, tumor formations excision may be improved by destroying more of the affected tissue rather than healthy tissue through magnetic drug targeted therapies. Worth noting, magnetic targeting has also industrial applications (*e.g.*, micro stirring devices) [4].

In this paper we focus on the analysis and optimization of a static magnetic field source (*e.g.*, a permanent magnet), able to generate a high gradient magnetic field, to obtain a localized and an as high as possible fluid flow – magnetic field interaction that may prolong the time of residence of the medication in the ROI. To this aim, we investigated, first, simpler two-dimensional idealized models (*e.g.*, channels, ducts) for the interaction of the aggregate fluid (blood *and* magnetic drug) with the magnetic field; next we turned our attention to more complex 3D models.

Finally, using the permanent magnet configuration found through this procedure, we investigate the flow – field interaction in a more realistic, medical image based model for the aorta and iliac arteries. To start with, the magnetic field source optimization process begins with the study of 2D models for the blood flow – magnetic field interaction analysis. Next, a more complex case described by an idealized 3D computational domain was considered. Finally, using the optimized array of magnets we studied the flow – magnetic field for a more realistic model, based on a 3D computational domain built out of medical image. The numerical simulations were performed in the finite element method (FEM) technique.

II. The Mathematical Model

In this study we neglect the flow-vessel walls structural interactions. Previous studies [6] revealed that, although a problem of concern in many circumstances, it is less so in magnetic drug targeting. The magnetic drug transport and fixation problem is analyzed by coupling the magnetic field model to the fluid flow. The aggregate fluid – blood and medication – has the magnetic properties of the drug carrier (a superparamagnetic material). First, the static magnetic field problem of the permanent magnet is solved for to find the (magnetization) body forces. Next, the fluid-flow interaction is studied. In this two-step approach we neglect the reaction of the flow upon the external magnetic field. The reason is the relatively low velocity field in hemodynamic.

A. The Magnetic Field Model

The magnetic field source is an array of permanent magnets. The magnetic field model is governed then by

Ampère's law

$$\nabla \times \mathbf{H} = 0 \tag{1}$$

Magnetic flux law

$$\nabla \cdot \mathbf{B} = 0 \tag{2}$$

Constitutive law for

$$\mathbf{B} = \mu_0 \mu_{r,mag} \mathbf{H} + \mathbf{B}_{rem} \text{ (permanent magnet)} \tag{3}$$

$$\mathbf{B} = \mu_0 \left[\mathbf{H} + \mathbf{M}_{ff}(\mathbf{H}) \right] \text{(aggregate fluid)} \tag{4}$$

$$\mathbf{B} = \mu_0 \mathbf{H} \text{ (elsewhere)} \tag{5}$$

S. Vlad and R.V. Ciupa (Eds.): MEDITECH 2011, IFMBE Proceedings 36, pp. 310–315, 2011.
www.springerlink.com

Here, μ_0 is the magnetic permeability of air; μ_r is the relative magnetic permeability of the permanent magnet; **H** is the magnetic field strength; **B** is the magnetic flux density; $\mathbf{B}_{rem}$ is the remanent magnetic flux density; and $\mathbf{M}_{ff}$ is the magnetization of the aggregate fluid, a function of **H**. Using the magnetic vector potential **A** (and the divergence free gauge condition)

$$\mathbf{B} = \nabla \times \mathbf{A}, \quad \nabla \cdot \mathbf{A} = 0, \tag{6}$$

the mathematical model for the magnetic field problem is

$$\nabla \times \left(\mu_0^{-1}\mu_r^{-1}\nabla \times \mathbf{A}\right) = 0. \tag{7}$$

The computational domain was conveniently extended (*i.e.*, the confining boundary was set "far away") such that magnetic insulation boundary conditions $(\mathbf{n} \times \mathbf{A} = 0)$ may be set. Alternatively, "infinite elements" may be used. Although this latter approach leads to computational domains of smaller sizes, hence fewer elements, the computational effort may be larger than acceptable.

B. The Hemodynamic Model

The magnetic fluid aggregate is assumed Newtonian, with constant properties, and its flow is incompressible and laminar [5], [6]. This approach is consistent with larger arteries, of "resistive" nature [11]. Different rheological models may be needed in different sections of the arterial tree. The flow model is described then by

momentum balance (*Navier-Stokes*)

$$\rho\left[\frac{\partial \mathbf{u}}{\partial t} + (\mathbf{u}\cdot\nabla)\mathbf{u}\right] = -\nabla\left[-p\mathbf{I} + \eta\left(\nabla\mathbf{u} + (\nabla\mathbf{u})^T\right)\right] + \mathbf{f}_{mg}, \tag{8}$$

mass conservation

$$\nabla \cdot \mathbf{u} = 0. \tag{9}$$

Here **u** is the velocity field, p is pressure, ρ is the mass density (1,060 kg/m^3]), η is the dynamic viscosity (0.005 Pa·s]), and **I** is the unity matrix. The magnetic body forces in eq. (8), due to the fluid aggregate magnetization in an external magnetic field, are given by $\mathbf{f}_{mg} = \mu_0(\mathbf{M}\cdot\nabla)\mathbf{H}$ [7]. We recall that the ensemble blood and magnetic drug carrier behaves as a magnetizable fluid that bears the magnetic properties of the material of which the magnetic nanoparticles are made of.

The boundary conditions that close the hemodynamic model are either constant or pulsatille inlet velocity, uniform pressure condition at the outlet(s), and no-slip (solid wall) conditions at the vessels walls. Mass transfer through the vessels walls is neglected in this study.

It should be mentioned that the magnetic field used in MDT is too small to impede the flow by interacting with the hematocrit and O_2 concentration in blood. In the absence of the magnetic particles used in MDT much higher magnetic flux densities are needed to influence the blood flow [12].

III. Magnetic field source optimization

Several arrays of permanent magnets were studied in order to find out the highest gradient magnetic field source structure.

A. 2D Models and Analysis

First, a simple 1 cm wide and 0.2 cm tall rectangular permanent magnet is considered. Then, nine configurations of permanent magnet arrays were studied. For each configuration three cases were analyzed. They were obtained by varying the magnets width (d_1) and the spacing (d_2), *i.e.* the aspect ratio (AR) d_1/d_2, while keeping the same overall dimensions of the array: height (0.2 cm) and total length (1 cm).

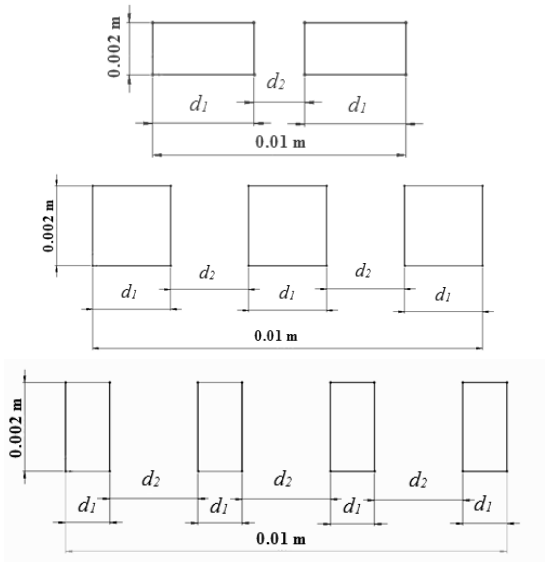

Fig. 1 The array of magnets in the 2D models: (a) 2; (b) 3; (c) 4 magnets

AR was varied between 0.4…5, and the arrays were used as magnetic field sources in the magnetic field – flow interaction 2D model.

The magnetic field model (7), solved first, provides the magnetic vector potential **A**. The magnetic body forces, $\mathbf{f}_{mg}$, are next determined, and used in the field-flow interaction model (8)-(9). Fig. 2 shows the 2D computational domain.

The numerical model (1) – (9) was implemented and numerically solved by Comsol FEM [8]. The simulation

results, for pulsatile flow conditions, were analyzed with the aim at finding the optimal array of magnets, judged by the associated magnetic body forces (*i.e.*, the magnetic field gradient). In this 2D model there are two components of $\mathbf{f}_{mg}$: the horizontal (Ox) component, $\mathbf{f}_{mg,x}$, opposite to the flow, and the vertical component (Oy), $\mathbf{f}_{mg,y}$, that attracts the aggregate fluid to the vessel wall. As the magnetic targeting effect is more significant during the minimum mass flow rate interval, we focus on this specific moment.

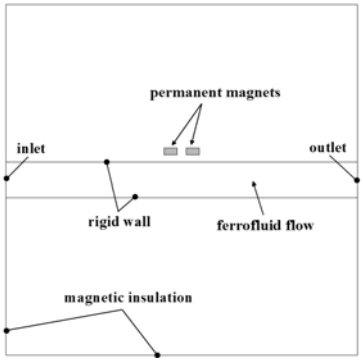

Fig. 2 The 2D computational domain and the boundary conditions

Both components are important: $\mathbf{f}_{mg,x}$ (parallel to the stream) acts into extending the time of residence of the aggregate fluid in the ROI (by slowing down the flow). The vertical component (orthogonal to the stream), $\mathbf{f}_{mg,y}$, enhances approach velocity to the vessel walls in the ROI. Both effects are more important during the low mass flow interval of the pulsating arterial flow. Fig. 3, 4 show the magnetic body forces at the wall.

They are averaged over the span of the magnet shadow (its projection on the upper wall of the channel, Fig. 2).

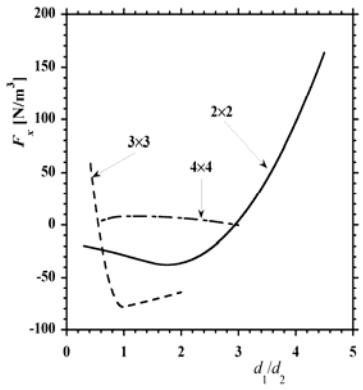

Fig. 3 The average magnetic body force $\mathbf{f}_{mg,x}$ for different arrays and ARs

Sure, at the wall, the flow velocity is zero (in virtue of the no-slip condition) but the magnetic forces reach here their upper (asymptotic) bounds. These values are used for comparison purposes.

The simulation results show that the larger the array the higher is the stream-wise gradient of the magnetic field whereas the vertical component does not vary significantly. We may then conjecture that the smallest array (2 magnets) may be an advisable choice. Moreover, increasing ARs – leading to a compact magnet – provides better design.

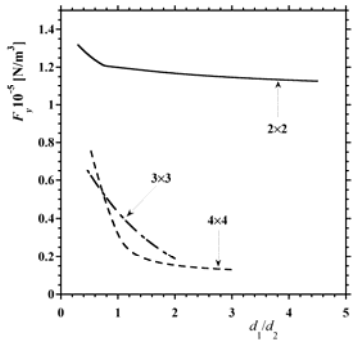

Fig. 4 The average magnetic body force $\mathbf{f}_{mg,y}$ for different arrays and ARs.

It is interesting to notice that the 4 magnets array gives a maximum stream-wise force with respect to the AR for $d_1 \sim d_2$. In what follows we look at these results in a 3D layout – for this notional flow geometry – to verify whether these 2D results are still valid.

B. 3D Models and Analysis

The three arrays (2×2, 3x3, 4x4 magnets), occupying the same 3D volume, were studied for different ARs. Fig. 5 shows the computational domain for a notional vessel with the 4x4 array of magnets. The non-magnetic mass that embeds the array is not shown here, for better view.

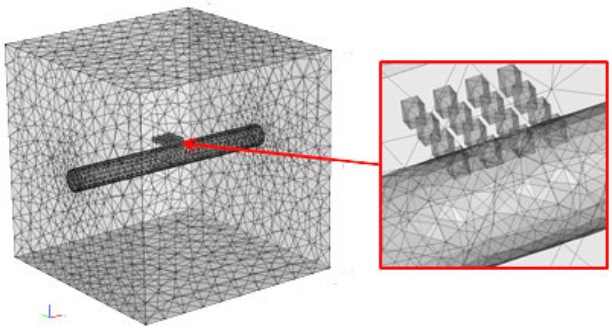

Fig. 5 The FEM mesh for the 4×4 array of magnets –3D notional model.

The mathematical model that describes the static magnetic field and the pulsating hydrodynamic flow coupled problems (1)–(9) were solved numerically [8]. The boundary conditions are consistent to the previous 2D models. The mass flow rate has the same time variation as in the 2D analysis

$$U_{in}(t) = U_0\left[\sin(\omega t) + \sqrt{\sin(\omega t)^2}\right], \qquad (10)$$

where U_0 = 50 cm/s, and $\omega = 2\pi f$ rad/s, f = 60 beats/minute.

The remanent flux density acts in the Oz direction, and the flow is in Ox direction. Oy direction, typical for 3D here, makes the difference between the 2D and 3D models.

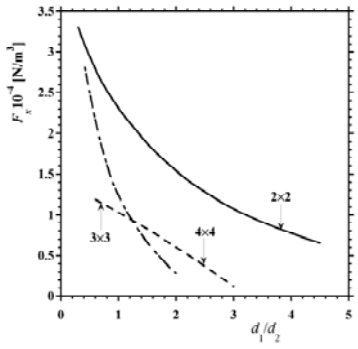

Fig. 6 The body force $\mathbf{f}_{mg,x}$ for different arrays and ARs – 3D models

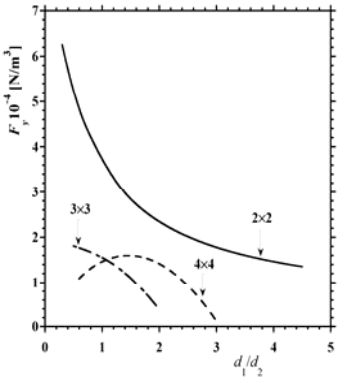

Fig. 7 The body force $\mathbf{f}_{mg,y}$ for different arrays and ARs – 3D models

In our study of the optimal magnet array we pursued the same steps, solving the problem for different ARs. The averaged body forces are shown in Fig. 6, 7, 8. Apparently, the 2×2 array provides for the best solution. However, the body forces decrease with increasing AR. This effect was noticed for the body force transversal to the walls (Fig. 4) in the previous 2D analysis. Here we note the same (decreasing) trend exhibited by the stream-wise component. This behavior, different in the 2D analysis (Fig. 3), may be explained by a 3D effect, not evidenced by the simpler 2D model. As expected, the d_1~d_2 case is best for the 2×2 array.

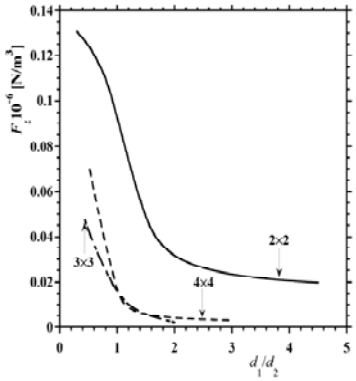

Fig. 8 The body force $\mathbf{f}_{mg,z}$ for different arrays and ARs – 3D models

The magnetic body force component (almost) perpendicular to the wall (responsible for conveying the drug to the vessel wall) has a knee for AR ~ 2. For values of AR less than 2 it exhibits a steep decrease with respect to AR, whereas for larger than 2 values of AR the decrease flattens. Apparently, for AR in the range 3…5 this component is almost constant.

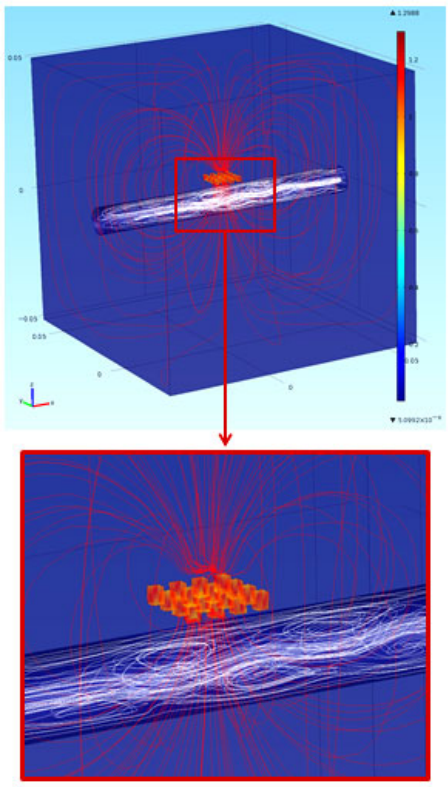

Fig. 9 The magnetic field and flow at the minimum mass flow rate. Recirculation areas build up and magnetic body forces may help conveying the medication to the ROI

It is interesting to notice that, as for the 2D analysis, the 4×4 array (16 permanent magnets, each 0.143 cm wide, equally spaced by 0.143 cm from each other) has a maximum at AR ~ 1 (d_1~d_2), when it provides its highest magnetic field gradient. This arrangement behaves almost as well as the 4x4 array in what concerns the stream-wise body force for lower values of AR.

Fig. 9 shows the magnetic field spectra (field lines and boundary surface map for the magnetic flux density) and the flow field (velocity streamlines) for the 4×4 array of magnets. A magnified view of the region where the magnet is located (presumably, nearby the region of therapeutic interest) provides details of the flow field. Recirculation is generated at every minimum mass flow rate. These particular moments provide for best conditions for the injected medication to diffuse in the therapeutic ROI.

IV. A MORE REALISTIC MODEL

To approach as closer as possible the medical procedure of the magnetically targeted drug transport and fixation a more realistic (*i.e.*, patient related) computational domain is needed. To this aim, we used a DICOM image set acquired by a MRI scanner. Fig. 10 shows several slices in the set that may provide the needed imagistic information. The ROI were segmented out and processed using a set of imagistic reconstruction tools [9].

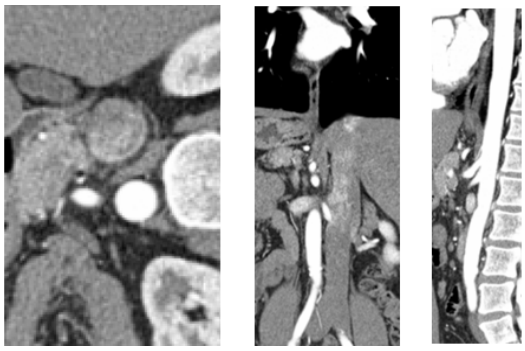

Fig. 10 Slices from a MRI DICOM set containing information about the human arteries in the chest and abdominal region that were used as source for the reconstruction process of the aorta and iliac 3D solid model

The computational "box" that contains the magneto-static problem of the 4×4 permanent magnet array (d_1=d_2) was generated using a CAD program [10] (Fig. 11). Particular care was devoted to model the magnetic array itself. During the meshing process the 16 permanent magnets may suffer unwanted edge fillet processes that would request a much too fine mesh to provide satisfactory numerical accuracy. We overcome this inconvenient by analytically modeling the 4×4 array. The model was FEM discretized (Fig. 12).

The blood vessel is part of the arterial tree called of "resistance" type with diameters in the range 20-25 mm [11], [6]. Therefore the pressures at the inlet and outlet flow ports may vary synchronously. We assume p_1 = 11,000 N/m^2, p_2 = 10,000 N/m^2, and p_3 = 10,000 N/m^2, where here $p_i(t) = p_i[1 + K\sin(t + 3/2)]$, i = {I, 2, 3}, and K is a factor of order 10^{-1} (here, K = 0.2).

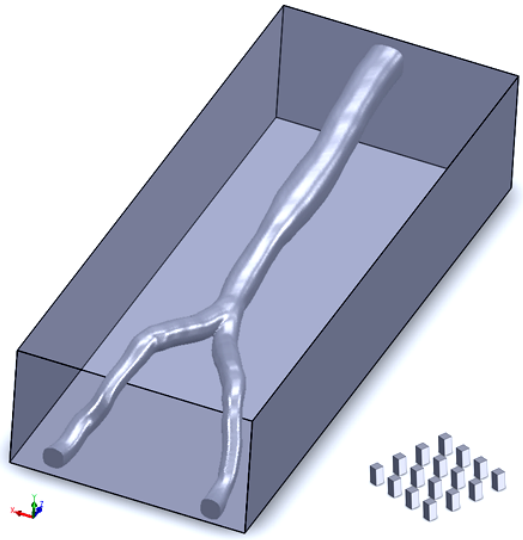

Fig. 11 The reconstructed 3D solid model of the arteries. The 4×4 array of magnets is shown (enlarged) aside. Only the magnets are shown

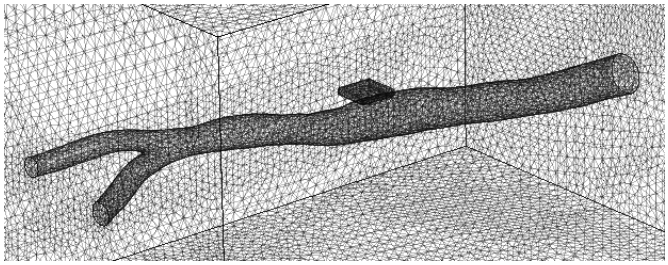

Fig. 12 The FEM mesh – *approx.* 265,000 Lagrange tetrahedral elements

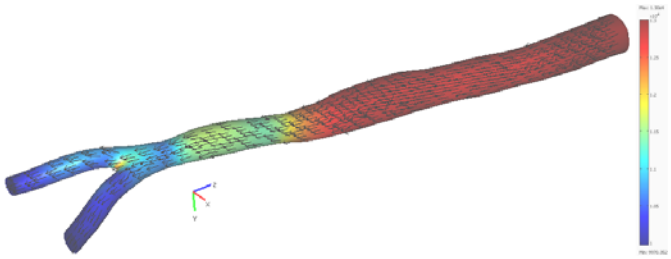

Fig. 13 The unperturbed, pulsating flow – at minimum mass flow rate

Fig. 13 shows the flow unperturbed by the magnetic field through velocity arrows and pressure surface color map. The non-zero average mass flow rate and the outlet conditions set for the downstream boundaries do not promote recirculation built up.

Fig. 14 shows the magnetic and the flow field at minimum mass flow rate. Here, although less effective than for the flow with zero mass flow rate intervals (section III, Fig. 9), the magnetic body forces do modify, locally, the flow pattern.

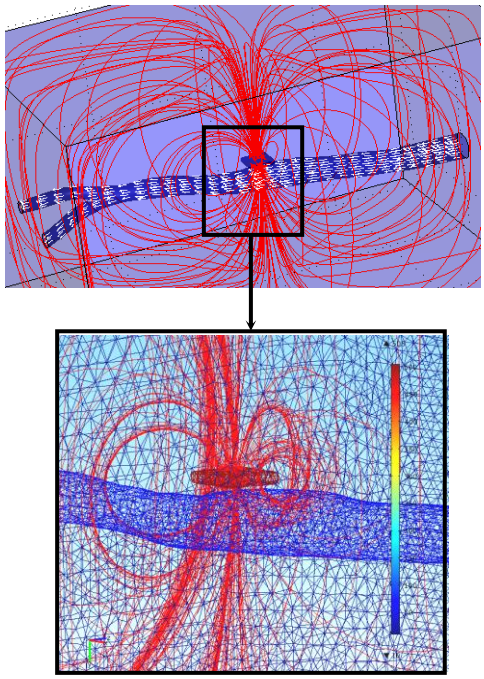

Fig. 14 The flow with magnetic field – at minimum mass flow rate

The investigation of this transport effect combined with the diffusion of medication through the vessel walls makes the object of a future research. In this study the drug that coats magnetic nanoparticles has not a distinct identity and it is rather dispersed in the blood stream.

V. Conclusions

Magnetic drug targeting (MDT) may be an invasive procedure therefore the design of the magnetic field source to best provide for medication delivery is of concern, and this paper reports numerical simulation results on its optimization. Different array-type of magnets were investigated, and compared based on the field gradient they produce. Apparently, the 2D and 3D models lead to different results, and it is suggested that the optimization (hence, the flow-field interaction itself) needs to be conducted on 3D models. Finally, to port these findings to a more realistic situation, a 3D model obtained out of patient specific MRI imagery for a segment of the arterial tree was built. The pulsating arterial flow – magnetic field was then investigated.

Acknowledgments

The work was conducted in the Laboratory for Electrical Engineering in Medicine (IEM) – Multiphysics Models, the BIOINGTEH platform at UPB, and it supported in part by POSDRU/88/1.5/S/61178 and CNCSIS PCCE-55/2008.

References

1. Alexiou C, Jurgons R, Schmid, RJ, Bergemann C, Henke J, Erhardt W, Huenges E, Parak F (2003) Magnetic drug targeting-biodistribution of the magnetic carrier and the chemotherapeutic agent mitoxantrone after locoregional cancer treatment, J. Drug Target. 11, 3:139-149.
2. Voltairas PA, Fotiadis DI, Michalis LK (2002) Hydrodynamics of Magnetic Drug Targeting, J. Biomech., 35:813–821.
3. Plavins J, Lauva M (1993) Study of Colloidal Magnetite Binding Erythrocytes: Prospects for Cell Separation, J. of Magnetism and Magnetic Materials, 122:349-353.
4. Suzuki H, (2003) Development of a Chaotic Micro-Mixer Using Magnetic Beads, PhD Thesis, UCLA, USA.
5. Morega AM, Dobre A, Morega M, Mocanu D (2009) Computational modeling of arterial blood flow, Proc. Second MediTech Conference, 23-26 September 2009, Cluj-Napoca, Romania.
6. Morega A M, Dobre AA, Morega M (2010) Numerical simulation of magnetic drug targeting with flow – structural interaction in an arterial branching region of interest, 17-19 Nov. 2010 Comsol Conference, Versailles, France
7. Rosensweig RE (1997) Ferrohydrodynamics, Dover Publications, NY
8. Comsol Multiphysics, v. 3.5a (2010), COMSOL A.B., Sweden.
9. Simpelware v. 3.2, Simpleware Ltd., UK, 2009.
10. SolidWorks (2009)
11. Feijóo RA (2000) Computational methods in biology, second Summer School LNCC/MCT, Petrópolis, January 2000.
12. Morega, A.M. and Morega, M. (2005) A FEM analysis of Magnetically induced biomagnetic fluid mixing, Rev. Roumaine Sci. Techn. Electrotech. et Energ., 50, 2:239-248.

Author: Alexandru M. MOREGA
Institute: University POLITEHNICA of Bucharest
Street: Splaiul Independenței, nr. 313, sector 6, 060042
City: Bucharest
Author: ROMANIA
E-mail: amm@iem.pub.ro